Journal Name

Supplementary Information for: Controlling Local Thermal Gradients at Molecular Scales with Janus Nanoheaters

Mingxuan Jiang[a] Aidan Chapman[a], Juan D. Olarte-Plata[a] and Fernando Bresme[a*]

1 Simulation Parameters

We used LAMMPS[1] (version 19Mar20) to run all the simulations, and for generating all spherical and cylindrical particles. Python 3.9.1 was used for data analysis. For the Atomistic Nodal Approach we calculated the per-atom heat flux, Voronoi volume (from the Voro++ package[2]), and atomistic temperature and positions using the per-atom averaging feature included in LAMMPS. The MD data was analysed using the Atomic Nodal Approach to obtain the local interfacial thermal conductance.

The following data-processing tools were used too: Ovito 3.5.2[3] (coordination analysis, α-shape), SciPy 1.6.0 LinearNDInterpolator library to obtain ΔT and Sklearn 0.24.1 for agglomerative clustering. The Atomic Simulation Environment (ASE) Package[4] and Ovito was used to generate the structures. Numpy 1.6.1 was used for general calculations as well. Dask 2.3.0 and pandas 1.1.3 are used for data handling and parallelising the code. The code is available on GitHub at `https://github.com/bresmegroup/Atomistic_Nodal_Approach_Nanoparticles`

All NP shapes generated have a density of $\rho^* \approx 1.0$, and a face-centered cubic (FCC) unit cell structure. We applied a hot thermostat $R^* = 2$ away from the surface, with a temperature of $T^* = 0.92$ and a cold thermostat $R^* = 7$ away from the particle surface, with a temperature of $T^* = 0.72$.

2 Sphere

We used a series of spherical shells with a $\delta R^* = 0.2$ to sample the properties of a Janus sphere. A sphere of radius of $R^* = 20.0$ was investigated to test the ANA and continuity equations, and to evaluate the interfacial thermal conductance of a Janus sphere. The size of the box was set to be a square box of length $l^* = 80$. We deployed 2 methods, both the bulk binning

approach (BBA)[5–7] and the atomistic nodal approach (ANA)[8]. The spherical nanoparticle was generated using the region-sphere function in LAMMPS.[1]

2.1 Atomistic Nodal Approach

We used the atomistic nodal approach as described previously in[8]. This method relies on computational farming of a thousand individual MD simulations, each with a different redistribution of the velocities in each simulation. Each individual simulation is a non-equilibrium MD simulation, and key thermodynamic data such as density, temperature and heat flux are collected on both a fine grid of the fluid and also per atom of the nanoparticle. Of special note is the heat flux, which is calculated using the Irving-Kirkwood evaluation:

$$\boldsymbol{J}_{q,i} = \frac{1}{V_i} \left[\frac{1}{2} m_i \boldsymbol{v}_i^2 \boldsymbol{v}_i + \phi_i \boldsymbol{v}_i + \frac{1}{2} \sum_{j \neq i} \left(\boldsymbol{v}_i \cdot \boldsymbol{F}_{ij} \right) \boldsymbol{r}_{ij} \right] \tag{1}$$

where $\boldsymbol{J}_{q,i}$ is the heat flux corresponding to particle i, with associated volume V_i calculated using the Voronoi polyhedra approach. The first term in equation (1) represents the kinetic energy flux of particle i and the second term its potential energy flux, where ϕ_i is the potential energy of particle i in the field of all the other particles. The third term, referred to as the collisional contribution, takes into account the flux contribution to the forces between particle i and j separated by a distance r_{ij}, and it is the dominant contribution in dense fluids and solids.

2.1.1 Nanorod

A nanorod of radius $R^* = 5.5$ (along y and z, perpendicular to the axial direction) and length $L^* = 20$ (along x, axial direction) was simulated in a rectangular cuboid box with lengths $l^* = 66.7$ (along x) and $b^* = 38.1$ (along y and z). The nanowire was generated by cutting 8 (110) and (100) planes out of an FCC lattice to form an octagonal rod.

[a] Department of Chemistry, Molecular Sciences Research Hub, Imperial College London, London, United Kingdom. Tel: 0044 207 594 5886; E-mail: f.bresme@imperial.ac.uk

2.2 Bulk Binning Approach

We applied the bulk binning approach to the spherical Janus nanoparticle. In the bulk binding approach, we obtained thermodynamic properties like heat flux, density and temperature from spherical shells centered at the nanoparticle center. These spherical shells spread radially outward, with a $\delta R^* = 0.2$ between each shell.

3 Temperature & Heat Flux Profiles for Janus NP

The validity of the continuity equations like Fourier's law of thermal conduction was evaluated both numerically and analytically:

$$\left.\frac{q_r}{A(r)}\right|_r = -\kappa\left.\frac{dT}{dr}\right|_r \tag{2}$$

Fourier's law states that the rate of heat transfer q_r over an area $A(r)$ is negatively proportional to the thermal conductivity κ of the material normal to the temperature gradient. Fourier's law can be verified, by sampling the radial heat flux $\frac{q_r}{A(r)}$ across various radii using the Irving-Kirkwood formula, and by examining its relationship with the numerical thermal gradient calculated from simulated data.

3.1 Continuity Equation for Nanospheres

For a sphere of radius R, Fourier's law be used to obtain a relationship between the radial distance r from a reference radius R_c and the temperature T difference from a reference point T_c.

$$\left.\frac{q_r}{A(r)}\right|_R = -\kappa\left.\frac{dT}{dR}\right|_R \tag{3}$$

$$\frac{q_r}{4\pi R^2}dR = -\kappa dT \tag{4}$$

$$\frac{q_r}{4\pi}\int_{R_c}^{R}\frac{dR}{R^2} = -\kappa\int_{T_c}^{T}dT \tag{5}$$

$$\frac{q_r}{4\pi}\left(\frac{1}{R}-\frac{1}{R_c}\right) = \kappa(T-T_c) \tag{6}$$

3.2 Using the Error function at the NP-Fluid Interface

To model the temperature transition between the NP $T_p(r)$ and fluid $T_F(r)$ or (R instead of r for nanospheres) and account for their different thermal conductivities κ_p and κ_l and the interfacial temperature "jump" we used an error function equation:

$$T(r) = \frac{1}{2}\left[T_p(r)+T_F(r)-\left(T_p(r)-T_F(r)\right)\text{erf}\left(\frac{\sqrt{\pi}(r-r_c)}{\omega}\right)\right] \tag{7}$$

Where r_c refers to the critical transition point, and ω quantifies the steepness of the error function $\text{erf}(\frac{\sqrt{\pi}(r-r_c)}{\omega})$. The temperature "jump" ΔT can be found using $\Delta T = T_p(r_c) - T_F(r_c)$, which is defined in terms of the temperature of the particle, T_c^p, and the fluid, T_c^F, at r_c.
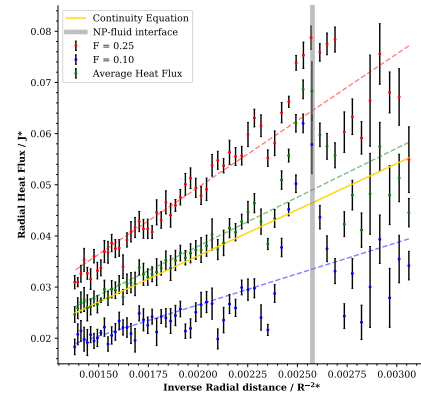
Fig. 1 Heat flux is inversely related to the surface area of the Janus NP sphere proportional to the $1/R^2$ with accordance to[5,9] for both sides of the Janus NP.
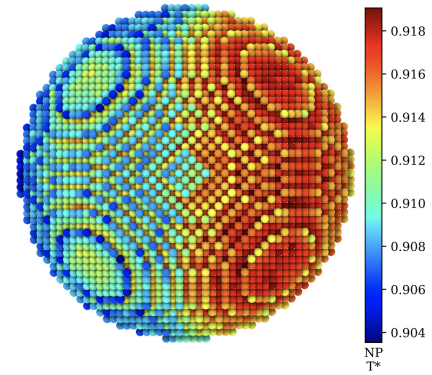
Fig. 2 Temperature of the Janus NP projected on the atomic coordinates of nanoparticle surface.
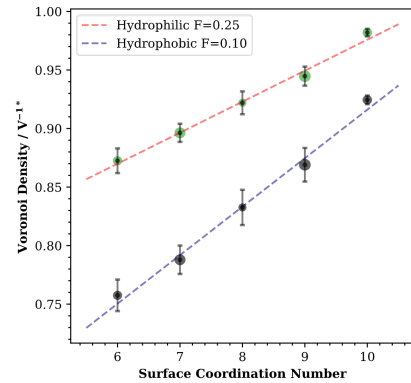
Fig. 3 Dependence of the Voronoi density with the coordination number of the atoms in the surface of the JNP. We show results for the philic ($F = 0.25$) and phobic regions ($F = 0.1$).

Notes and references

1 S. Plimpton, *Journal of computational physics*, 1995, **117**, 1–19.
2 C. H. Rycroft, *Chaos: An Interdisciplinary Journal of Nonlinear Science*, 2009, **19**, 041111.
3 A. Stukowski, *Modelling and Simulation in Materials Science and Engineering*, 2010, **18**, 015012.

(a)

(b)
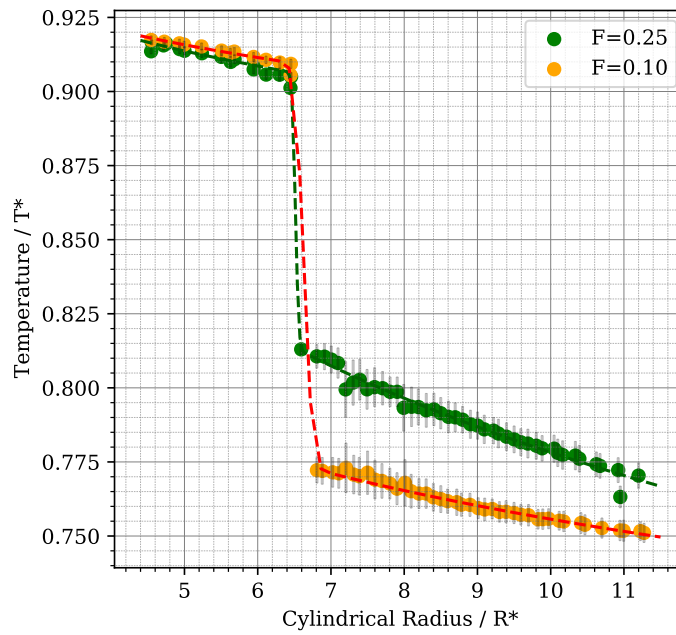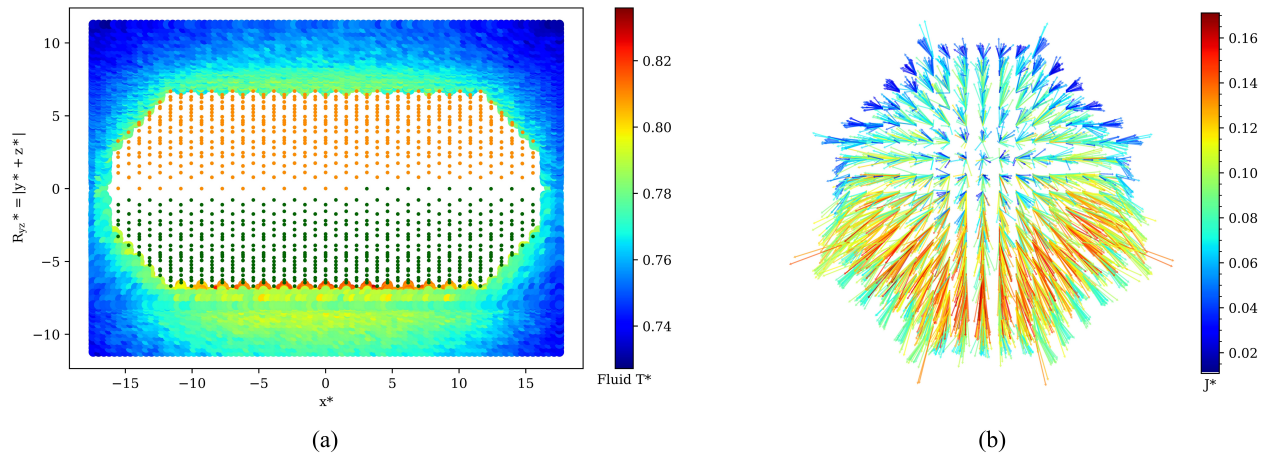
Fig. 4 (a) Fluid temperature T^* and distribution around the Janus nanorod. (b) Heat flux of the Janus nanorod. Both the fluid temperature and heat flux indicate significant anisotropic character along one side of the NP. (Bottom panel) Radial temperature profile around the main axis of the Janus nanorod.

CN	δ Density ρ^*	δ Conductance G^*	δ NP Temp $T*$	δ Fluid 1st Shell Temp $T*$
6	1.19 ± 0.04	0.73 ± 0.03	2.3 ± 0.1	4.18 ± 0.07
7	0.94 ± 0.04	0.80 ± 0.04	2.7 ± 0.1	4.24 ± 0.7
8 (Sphere)	1.08 ± 0.06	1.35 ± 0.08	2.2 ± 0.1	4.27 ± 0.09
8 (Rod +)	1.19 ± 0.06	1.2 ± 0.1	2.3 ± 0.6	3.0 ± 0.3
8 (Rod -)	0.91 ± 0.03	0.95 ± 0.07	2.5 ± 0.6	3.1 ± 0.3
9	0.96 ± 0.07	1.4 ± 0.1	2.7 ± 0.1	3.3 ± 0.1
10	0.53 ± 0.06	1.7 ± 0.2	3.1 ± 0.2	3.94 ± 0.07

Table 1 Interfacial widths δ of the various C.N. measured for various physical properties, showing the extent of boundary effects between F=0.25 and F=0.10 on the physical properties of two types of Janus NP. For the Janus rod, the interfacial width for $z^* > 0$ is labelled as Rod +, while for $z^* < 0$, the interfacial widths are labelled as Rod -, to distinguish them from C.N.=8 for the Janus sphere.

4 A. H. Larsen, J. J. Mortensen, J. Blomqvist, I. E. Castelli, R. Christensen, M. Dułak, J. Friis, M. N. Groves, B. Hammer, C. Hargus, E. D. Hermes, P. C. Jennings, P. B. Jensen, J. Kermode, J. R. Kitchin, E. L. Kolsbjerg, J. Kubal, K. Kaasbjerg, S. Lysgaard, J. B. Maronsson, T. Maxson, T. Olsen, L. Pastewka, A. Peterson, C. Rostgaard, J. Schiøtz, O. Schütt, M. Strange, K. S. Thygesen, T. Vegge, L. Vilhelmsen, M. Walter, Z. Zeng and K. W. Jacobsen, *Journal of Physics: Condensed Matter*, 2017,

Component	r/Å	T_c/K	T_e/K	ω/Å	l_c/Å	δ/Å	$T_{c,\,err}$/K	$T_{e,\,err}$/K	ω_{err}/Å	$l_{c,\,err}$/Å	δ_{err}/Å
thiols	27	363.3	341.2	8.07	41.47	3.22	0.3692	0.3593	1.106	0.298	0.4411
thiols	28	360.7	338.6	13.06	45.09	5.209	0.462	0.4605	2.214	1.209	0.8832
thiols	29	360.3	337.5	5.508	43.91	2.197	0.3654	0.3367	0.7028	0.1993	0.2804
thiols	30	358.8	335.8	11.48	45.9	4.581	0.376	0.3658	2.297	1.38	0.9164
thiols	31	357.7	333.7	5.9	47.13	2.354	0.3108	0.2923	0.6552	0.1837	0.2614
thiols	32	356.1	331.6	12.43	50.33	4.958	0.3764	0.3726	1.505	0.9135	0.6005
thiols	33	354.2	328.8	6.444	50.19	2.571	0.3145	0.2987	0.702	0.1922	0.2801
water	36	314.1	320.8	34.3	46.49	13.68	0.3395	0.2386	7.773	2.043	3.101
water	41	311.9	316.6	29.54	60.27	11.78	0.07144	0.06464	2.498	0.691	0.9966
water	46	309.8	313.6	41.06	66.35	16.38	0.08023	0.07241	3.784	1.2	1.509
water	51	308.1	311.1	38.18	70.86	15.23	0.05734	0.04731	3.591	1.093	1.433
water	56	306.7	309	28.94	71.91	11.55	0.06056	0.04478	4.718	1.175	1.882
water	61	305.6	307.5	25.81	80.34	10.3	0.05967	0.04948	5.409	1.733	2.158
water	66	304.7	306.2	18.59	83.19	7.417	0.0769	0.06093	7.057	2.032	2.816

Table 2 Fitting parameters corresponding to the dotted lines in Figures 7a and 7b of the main text.
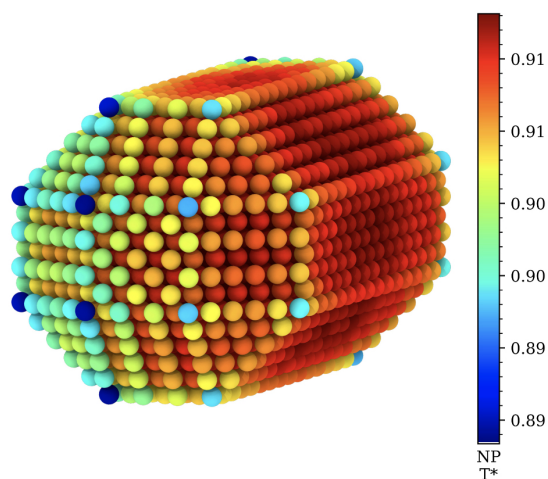
Fig. 5 NP temperature distribution T^* projected on the atomic coordinates of the surface atoms of the nanorod.

29, 273002.

5 A. S. Tascini, J. Armstrong, E. Chiavazzo, M. Fasano, P. Asinari and F. Bresme, *Physical Chemistry Chemical Physics*, 2017, **19**, 3244–3253.

6 S. M. Neidhart and J. D. Gezelter, *The Journal of Physical Chemistry C*, 2018, **122**, 1430–1436.

7 A. Rajabpour, R. Seif, S. Arabha, M. M. Heyhat, S. Merabia and A. Hassanali, *The Journal of chemical physics*, 2019, **150**, 114701.

8 M. Jiang, J. D. Olarte-Plata and F. Bresme, *The Journal of Chemical Physics*, 2022, **156**, 044701.

9 K. Jiang, D. A. Smith and A. Pinchuk, *The Journal of Physical Chemistry C*, 2013, **117**, 27073–27080.

(a) (b) (c)
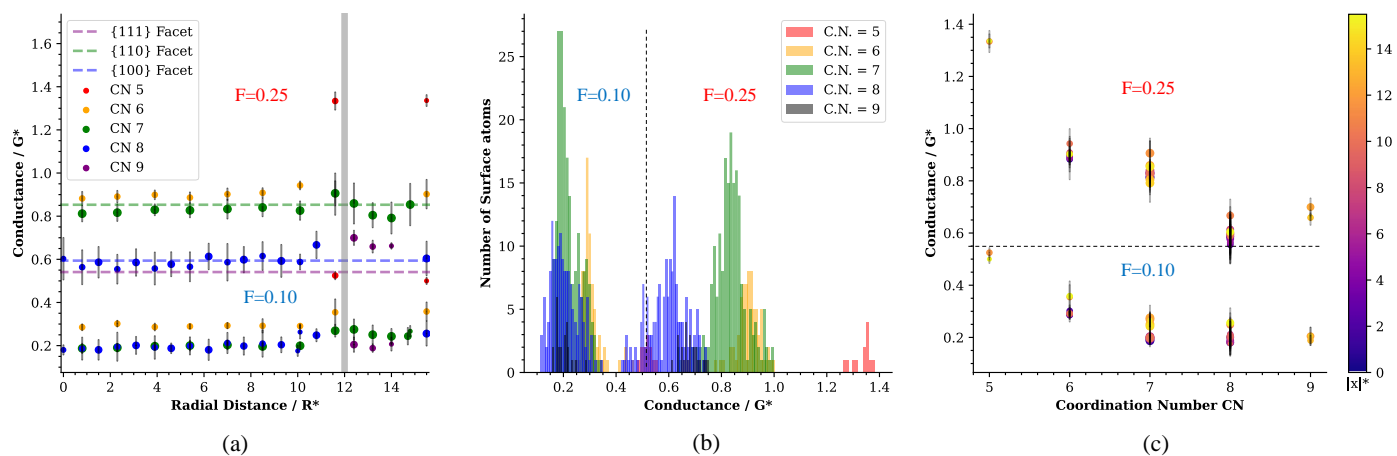
Fig. 6 (a) Changes in Conductance with radial distance. (b) Distribution of conductance value for surface atoms. (c) Variation of conductance with the coordination number.

(a) (b)
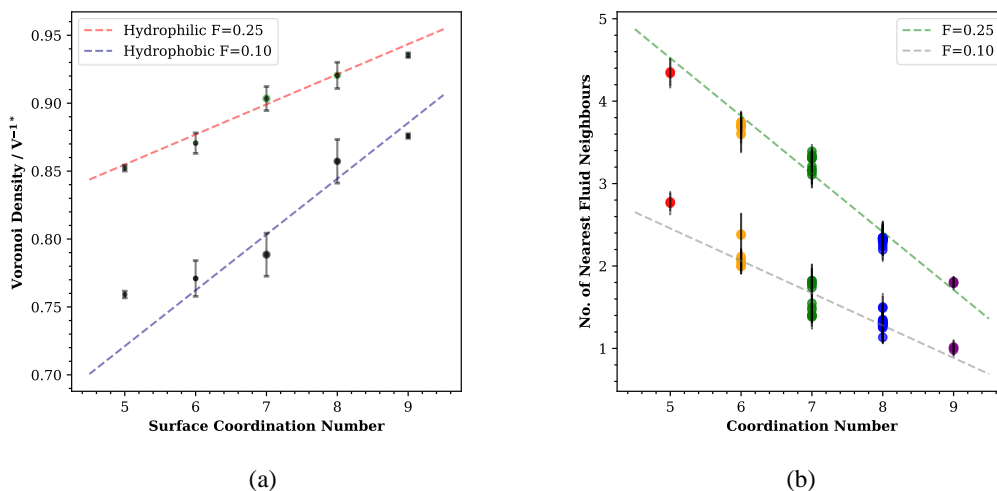
Fig. 7 (a) Variation of Voronoi density with coordination number shows a positive correlation but deviation from a linear relationship (b) Negative correlation between C.N. and number of first shell fluid atoms.
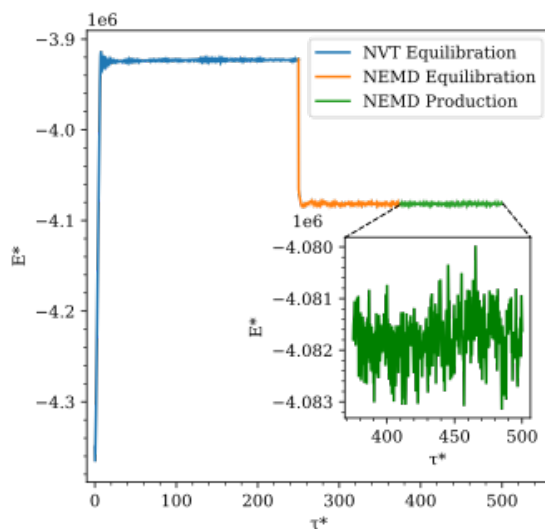
Fig. 8 Internal energy as a function of time, for a representative simulation. The panel illustrates the energy conservation during the NVT and NEMD equilibration and production phases.